

---

# Overcoming Distribution Mismatch in Quantizing Image Super-Resolution Networks

---

**Cheemun Hong**

Dept. of ECE & ASRI,  
Seoul National University  
cheemun914@snu.ac.kr

**Kyoung Mu Lee**

IPAI, Dept. of ECE & ASRI,  
Seoul National University  
kyoungmu@snu.ac.kr

## Abstract

Quantization is a promising approach to reduce the high computational complexity of image super-resolution (SR) networks. However, compared to high-level tasks like image classification, low-bit quantization leads to severe accuracy loss in SR networks. This is because feature distributions of SR networks are significantly divergent for each channel or input image, and is thus difficult to determine a quantization range. Existing SR quantization works approach this distribution mismatch problem by dynamically adapting quantization ranges to the variant distributions during test time. However, such dynamic adaptation incurs additional computational costs that limit the benefits of quantization. Instead, we propose a new quantization-aware training framework that effectively **Overcomes the Distribution Mismatch** problem in SR networks without the need for dynamic adaptation. Intuitively, the mismatch can be reduced by directly regularizing the variance in features during training. However, we observe that variance regularization can collide with the reconstruction loss during training and adversely impact SR accuracy. Thus, we avoid the conflict between two losses by regularizing the variance only when the gradients of variance regularization are cooperative with that of reconstruction. Additionally, to further reduce the distribution mismatch, we introduce distribution offsets to layers with a significant mismatch, which either scales or shifts channel-wise features. Our proposed algorithm, called ODM, effectively reduces the mismatch in distributions with minimal computational overhead. Experimental results show that ODM effectively outperforms existing SR quantization approaches with similar or fewer computations, demonstrating the importance of reducing the distribution mismatch problem. Our code is available at <https://github.com/Cheemun/ODM>.

## 1 Introduction

Image super-resolution (SR) is a core low-level vision task that aims to reconstruct the high-resolution (HR) images from their corresponding low-resolution (LR) counterparts. Recent advances in deep learning [10, 28, 33, 46, 47] have led to astonishing achievements in producing high-fidelity images. However, the remarkable performance relies on heavy network architectures with significant computational costs, which limits the practical viability, such as mobile deployment.

To mitigate the computational complexity of neural networks, quantization has emerged as a promising avenue. Network quantization has proven effective in reducing computation costs without much loss in accuracy, particularly in high-level vision tasks, such as image classification [7, 18, 49]. Nonetheless, when it comes to quantizing SR networks to lower bit-widths, a substantial performance degradation [22] occurs, posing a persistent and challenging problem to be addressed.

Such degradation can be attributed to the significant variance present in the activation (feature) distributions of SR networks. The feature distribution of a layer exhibits substantial discrepancies

across different channels and images, which makes it difficult to determine a single quantization range for a layer. Early approach on SR quantization [30] adopts quantization-aware training to learn better quantization ranges. However, as observed in Figure 1, despite careful selection, the quantization ranges fail to align with the diverse values within the channel and image dimension, which we refer to as *distribution mismatch*.

Recent approaches aim to address this challenge by incorporating dynamic adaptation methods to accommodate the varying distributions. For instance, DAQ [17] leverages distribution mean and variance to dynamically adjust quantization ranges for each channel and DDTB [48] employs input-adaptive dynamic modules to determine quantization ranges on a per-image basis. However, both channel-wise quantization ranges and dynamic adaptation modules introduce significant computational overhead. While adapting the quantization function to each image during inference might handle the variable distributions, it compromises the computational benefits of quantization.

In this study, we propose a novel quantization-aware training framework that addresses the distribution mismatch problem, by introducing a new loss term that regulates the variance in distributions. While direct regularization of distribution variance demonstrates potential in reducing quantization errors in each quantized feature, its relationship with the reconstruction loss is questionable. We observe that concurrently optimizing the network with variance regularization and reconstruction loss can disrupt the image reconstruction process, as shown in Figure 2. Therefore, we introduce a cooperative variance regularization strategy, where the variance is regulated only when it collaborates harmoniously with the reconstruction loss. To determine the cooperative behavior, we assess whether the sign values of the gradients from each loss are the same. Consequently, we can effectively update the SR network to optimize both quantization-friendliness and reconstruction accuracy.

To further reduce the distribution mismatch in SR networks, we introduce the concept of distribution offsets for features that exhibit severe mismatch. We first observe that the distribution mismatch problem is more critical in the channel dimension compared to the image dimension (Figure 1). Moreover, we find that the degree of channel-wise mismatch varies across different convolutional layers. As shown in Figure 3, certain layers exhibit a large mismatch between the distribution means, while others show a large mismatch between the distribution deviations. Intuitively, the mismatch in distribution mean can be reduced by applying channel-wise shifting of the distributions and that of the deviation be reduced by scaling. On this basis, we leverage additional offset parameters that either shift or scale the channel-wise distributions based on the specific mismatch aptitude of the layer. While these selectively-applied offsets effectively mitigate the distribution mismatch, they only incur negligible overhead, around  $\times 30$  smaller storage size overhead or  $\times 100$  fewer BitOPs compared to existing works with dynamic modules.

The contributions of our work include:

- We introduce the first quantization framework to address the distribution mismatch problem in SR networks without dynamic modules. Our framework updates the SR network to be quantization-friendly and accurate at the same time.
- We identify the distinct distribution mismatch among different layers and further reduce the distribution mismatch by shifting or scaling largely mismatching features.
- Compared to existing approaches on SR quantization, ours achieves state-of-the-art performance with similar or less computations.

## 2 Related Works

**Image super-resolution.** Convolutional neural network (CNN) based approaches [29, 33] have exhibited remarkable advancements in image super-resolution (SR) task, but at the cost of substantial computational resources. The massive computations of SR networks have led to a growing interest in developing lightweight SR architectures [9, 21, 20, 46, 25]. Furthermore, various lightweight networks are investigated through neural architecture search [8, 27, 31, 39, 32], knowledge distillation [20, 21, 45], and pruning [38]. While these methods mostly focus on reducing the network depth or the number of channels, our focus in this work is to lower the precision of floating-point operations with network quantization.

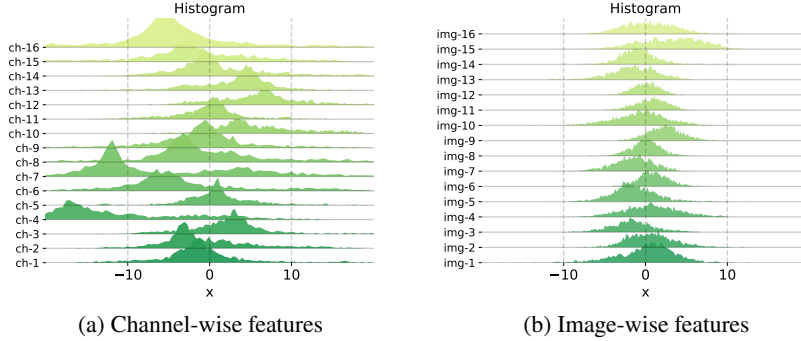


Figure 1: **Distribution mismatch in SR networks.** SR networks exhibit a large mismatch inside the feature distributions, which results in a large quantization error. The mismatch is observed in both channel-dimension and image-dimension, but channel-wise mismatch is larger in magnitude and also more critical. Channels and images of a layer are randomly selected for visualization.

**Network quantization.** By mapping 32-bit floating point values of input features and weights of convolutional layers to lower-bit values, network quantization provides a dramatic reduction in computational resources [6, 7, 13, 26, 49, 50]. Recent works successfully quantize various networks with low bit-widths without much compromise in network accuracy [5, 11, 15, 24, 35, 41, 44]. However, these works primarily focus on high-level vision tasks, while networks for low-level vision tasks remain vulnerable to low-bit quantization.

**Quantized super-resolution networks.** In contrast to high-level vision tasks, super-resolution poses different challenges due to inherently high accuracy sensitivity to quantization [22, 36, 43, 40]. A few works have attempted to recover the accuracy by modifying the network architecture [2, 23, 43] or by adopting different bits for each image [16] or network stage [34]. However, the key challenge of quantizing SR networks is in the vastly distinct feature distributions of SR networks. To deal with such issue, PAMS [30] adopts a learnable quantization range for different layers. More recently, DAQ [17] recognizes that the distributions are not only distinct per layer, but per channel and per input image and adopts dynamic quantization function for each channel. Moreover, DDTB [48] employs an input-adaptive dynamic module to adapt the quantization ranges differently for each input image. However, these dynamic adaptations of quantization functions during test-time cost non-negligible computational overheads. In contrast, instead of designing input-adaptive or channel-wise different quantization modules, we focus on mitigating the feature variance itself. Our framework reduces the inherent distribution mismatch in SR networks with minimal overhead, obtaining quantized networks without the need for dynamic modules.

### 3 Proposed method

#### 3.1 Preliminaries

To reduce the heavy computations of convolutional layers in neural networks, the input feature (activation) and weight of each convolutional layer are quantized to low-bit values [6, 7, 26, 14]. In this work, as the features of SR network are more sensitive to quantization, we focus more on quantizing features. The input feature of the  $i$ -th convolutional layer  $x_i \in \mathbb{R}^{B \times C \times H \times W}$ , where  $B, C, H$ , and  $W$  denote the dimension of input batch, channel, height, and width, a quantization operator  $Q(\cdot)$  quantizes the feature  $x_i$  with bit-width  $b$ :

$$Q(x_i) = \text{Int}\left(\frac{\text{clip}(x_i, \alpha_l, \alpha_u) - \alpha_l}{s}\right) \cdot s + \alpha_l, \quad (1)$$

where  $\text{clip}(\cdot, \alpha_l, \alpha_u)$  truncates the input into the range of  $[\alpha_l, \alpha_u]$  and  $s = \frac{\alpha_u - \alpha_l}{2^b - 1}$ . After truncation, the truncated feature is scaled to the integer range of bit-width  $b$ ,  $[0, 2^b - 1]$ . Then the scaled feature in the integer range is rounded to integer values with  $\text{Int}(\cdot)$ , and it is rescaled to range  $[\alpha_l, \alpha_u]$ . To obtain better quantization ranges for SR networks, range parameters  $\alpha_l, \alpha_u$  for each layer are generally

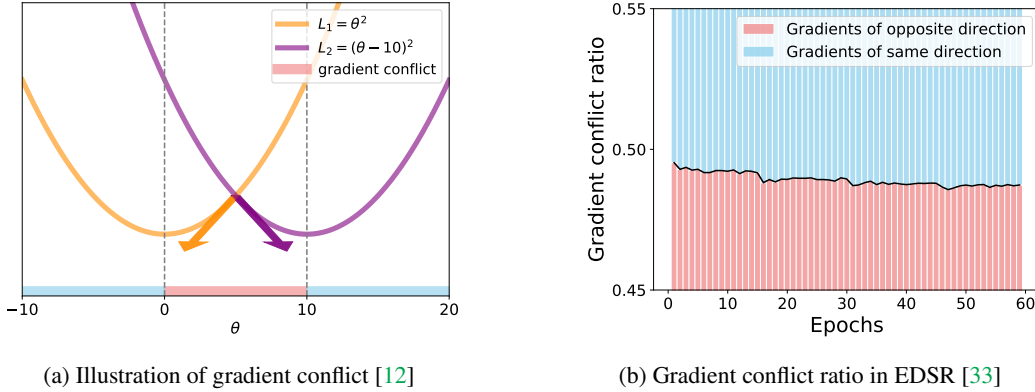


Figure 2: **Conflict between variance regularization and reconstruction loss.** Variance regularization updates a number of parameters in the *opposite* direction of reconstruction loss, which we refer to as gradient conflict. We plot the ratio of conflicted gradients during training when the two losses are jointly used. Nearly half of the parameters undergo gradient conflict and the ratio persists throughout training. This indicates that simply leveraging variance regularization and the reconstruction loss together can limit SR accuracy.

learned through quantization-aware training [30, 48]. Since the rounding function is not differentiable, a straight-through estimator (STE) [3] is used to train the range parameters in an end-to-end manner. We initialize  $\alpha_u$  and  $\alpha_l$  as the  $j$ -th and  $100 - j$ -th percentile value of feature averaged among the training data.  $j$  is set as 1 in our experiments to avoid outliers from corrupting the quantization range. Similarly, to quantize the weight of the  $i$ -th convolutional layer  $w^i$ , quantization operator  $Q(\cdot)$  is used. However, instead of setting range parameters as learnable parameters,  $\alpha_l, \alpha_u$  for weights are fixed as the  $j$ -th and  $100 - j$ -th percentile of weights.

### 3.2 Distribution mismatch in SR networks

Quantization unfriendliness of SR networks is from the diverse feature (activation) distributions, as reported in previous studies [30, 17, 48], mainly due to the absence of batch normalization layers in SR networks. Existing SR quantization methods address this issue by employing one [30] or two [48] learnable quantization range parameters for each convolutional layer feature. However, despite that the quantization-aware training process aims to find the optimal range for each feature, it fails to account for the channel-wise and input-wise variance in distributions. As illustrated in Figure 1, where notable discrepancies exist between layer-wise and channel-wise distributions, quantization grids are needlessly allocated to regions with minimal feature density. This mismatch in inter-channel distributions leads to performance degradation when quantizing SR networks. In the following sections, we introduce a new quantization-aware training scheme to address the distribution mismatch problem.

### 3.3 Cooperative variance regularization

Instead of focusing on finding a better quantization range parameter capable of accommodating the diverse feature distributions, our approach aims to regularize the distribution diversity beforehand. Obtaining an appropriate quantization range for a feature with low variance is an easier task compared to that of high variance. In this work, we define the overall mismatch of a feature distribution with the standard deviation,

$$M(x_i) := \sigma(x_i), \quad (2)$$

where  $\sigma(\cdot)$  calculates the standard deviation of the feature. Thus, variance regularization can be directly applied to the feature to be quantized ( $x_i$ ), which is formulated as follows:

$$\mathcal{L}_V(x_i) = \lambda_V \cdot M(x_i), \quad (3)$$

where  $\lambda_V$  is the hyperparameter that denotes the weight of regularization. The overall  $\mathcal{L}_V = \sum_i^{\# \text{ layers}} \mathcal{L}_V(x_i)$  is obtained by summing over all quantized convolutional layers. The variance regularization loss can be used in line with the reconstruction loss, which is originally used in the general

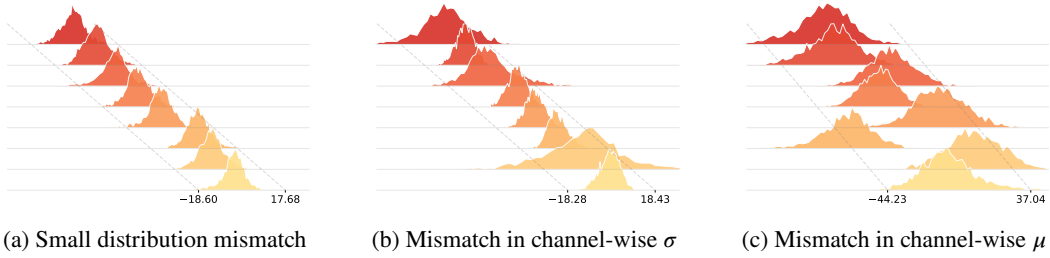


Figure 3: **The distribution mismatch of different layers in EDSR [33]**. While layer (a) shows an overall small mismatch between channels, layer (b) shows a large mismatch on deviation, and layer (c) exhibits a large mismatch on average. This motivates us to selectively *scale* features with large deviation mismatch ( $M_\sigma$ ) and *shift* features with a large average mismatch ( $M_\mu$ ).

quantization-aware training process. The optimization of parameter  $\theta^t$  is formulated as follows:

$$\theta^{t+1} = \theta^t - \alpha^t (\nabla_{\theta} \mathcal{L}_R(\theta^t) + \nabla_{\theta} \mathcal{L}_V(\theta^t)), \quad (4)$$

where  $\nabla_{\theta} \mathcal{L}_R(\theta^t)$  the gradient from the original reconstruction loss and  $\nabla_{\theta} \mathcal{L}_V(\theta^t)$  denotes the gradient from variance regularization loss and  $\alpha^t$  denotes the learning rate. Updating the network to minimize the variance regularization loss will reduce the quantization error of each feature.

However, then a question arises, *does reducing the quantization error of each feature lead to improved reconstruction accuracy?* The answer is, according to our observation in Figure 2, not necessarily. During the training process, the variance regularization loss can collide with the original reconstruction loss. However, we want to avoid the conflict between two losses, in other words, minimize the variance as long as it does not hinder the reconstruction loss. Thus, we determine whether the two losses are cooperative or not by examining the sign of the gradients of each loss. If the signs of the gradients are equal, then the parameter is updated in the same direction by two losses. By contrast, if the sign values are inverse, the two losses restrain each other, thus we only employ the reconstruction loss. In summary, we leverage variance regularization for parameters that the gradients have the same sign value as that from the reconstruction loss. Our optimization can be formulated as follows:

$$\theta^{t+1} = \begin{cases} \theta^t - \alpha^t (\nabla_{\theta} \mathcal{L}_R(\theta^t) + \nabla_{\theta} \mathcal{L}_V(\theta^t)), & \nabla_{\theta} \mathcal{L}_R(\theta^t) \cdot \nabla_{\theta} \mathcal{L}_V(\theta^t) \geq 0, \\ \theta^t - \alpha^t (\nabla_{\theta} \mathcal{L}_R(\theta^t)), & \nabla_{\theta} \mathcal{L}_R(\theta^t) \cdot \nabla_{\theta} \mathcal{L}_V(\theta^t) < 0. \end{cases} \quad (5)$$

This allows the network to reduce the quantization error cooperatively with the reconstruction error.

### 3.4 Distribution offsets

The variance of the distribution can be reduced to a certain extent via variance regularization in Section 3.3. However, since regularization is applied only when it is cooperative with the SR reconstruction, the gap between distributions remains. In this section, we explore the remaining gap between distributions. First, as visualized in Figure 1, we observe that the distribution gap is larger (and more critical) in the channel dimension compared to the image dimension.

Also, we find that this extent of the channel-wise gap in the distribution is different for each layer of the SR network, as shown in Figure 3. Some layers (Figure 3b) exhibit a larger mismatch in the distribution deviation, while others (Figure 3c) show a larger mismatch in the distribution average. The quantization errors of the layer with a large mismatch in distribution mean can be decreased by shifting the channel-wise feature. On the other hand, the mismatch in layers with large divergence in distribution deviation can be reduced by scaling each channel-wise distribution for overall similar distributions.

Since channel-wise shifting and scaling incur computational overhead and not all layers are in need of additional shifting and scaling (Figure 3a), we selectively apply offset scaling/shifting to layers that can maximally benefit from it. The standards for our selection are derived by feeding a patch of images to the 32-bit pre-trained network and calculating the mismatch in average/deviation of each layer. Given the  $i$ -th feature statistics  $\hat{x}^i$  from the pre-trained network, the mismatch of  $i$ -th convolutional layer is formulated as follows:

$$M_\mu^i := \sigma(\mu_c(\hat{x}_i)) \quad \text{and} \quad M_\sigma^i := \sigma(\sigma_c(\hat{x}_i)), \quad (6)$$

---

**Algorithm 1** Quantization-aware training process of ODM

---

**Input:** Pre-trained 32-bit network  $\mathcal{P}$ , distribution offset ratio  $p$ .

**Output:** Quantized network  $\mathcal{Q}$ .

Using  $\mathcal{P}$ , obtain  $M_\mu^i$  and  $M_\sigma^i$  ( $i = 1, \dots, \text{\#layers}$ ) using Eq. (6)

**for**  $i = 1, \dots, \text{\# layers}$  **do**

    Initialize quantization range parameters  $\alpha_l, \alpha_u$  for feature  $x_i$  of  $\mathcal{Q}$  using percentile

**if**  $M_\mu^i$  is in top- $p$  ratio among  $M_\mu^i$ s **then**

        Shift  $x_i$  with  $S_\mu$  using Eq. (7)

**if**  $M_\sigma^i$  is in top- $p$  ratio among  $M_\sigma^i$ s **then**

        Scale  $x_i$  with  $S_\sigma$  using Eq. (8)

    Given  $x_i$ , obtain variance regularization loss  $\mathcal{L}_V(x_i)$  using Eq. (3)

    Given  $\mathcal{L}_V$  and  $\mathcal{L}_1$ , update parameters of  $\mathcal{Q}$  using Eq. (5)

---

where  $\mu_c(\cdot)$  and  $\sigma_c(\cdot)$  respectively calculate the channel-wise mean and standard deviation of a feature and  $\sigma(\cdot)$  calculates the standard deviation. After all  $M_\mu^i$ s and  $M_\sigma^i$ s ( $i = 1, \dots, \text{\#layers}$ ) are collected, we apply additional scaling offsets to top- $p$  layers with high  $M_\sigma^i$  value and shifting offsets to top- $p$  layers with high  $M_\mu^i$  value. The shifting and scaling process for feature  $x^i$  of the  $i$ -th convolutional layer is formulated as follows:

$$x_i^* = x_i + S_\mu, \quad \text{if } M_\mu^i \in \text{top-}p([M_\mu^1, \dots, M_\mu^{\text{\#layers}}]), \quad (7)$$

$$x_i^* = x_i \cdot S_\sigma, \quad \text{if } M_\sigma^i \in \text{top-}p([M_\sigma^1, \dots, M_\sigma^{\text{\#layers}}]), \quad (8)$$

where  $S_\mu, S_\sigma \in \mathbb{R}^C$  are learnable parameters,  $\text{top-}p(\cdot)$  constructs a set that contains values greater than the  $100(1-p)$ -percentile value of the given set.  $p$  is the hyperparameter that determines the ratio of layers to apply distribution offsets, which we set to 0.3 in our experiments. Moreover, both offsets  $S_\mu$  and  $S_\sigma$  are quantized to low-bit, 4-bit in our experiments, to minimize the computational overhead. Consequently, the offsets additionally incur only 0.02% overhead to the network storage size for EDSR. The offsets further relieve distribution mismatch with minimal overhead.

### 3.5 Overall training

Algorithm 1 summarizes the overall pipeline for our framework, ODM. We follow the common practice [30, 48] to use  $\mathcal{L}_1$  loss and  $\mathcal{L}_{\text{SKT}}$  loss for the reconstruction loss as follows:

$$\mathcal{L}_R = \mathcal{L}_1 + \lambda \mathcal{L}_{\text{SKT}}, \quad (9)$$

where  $\mathcal{L}_1$  loss indicates the  $l_1$  distance between the reconstructed image and the ground-truth HR image, and  $\mathcal{L}_{\text{SKT}}$  loss is the  $l_2$  distance between the structural features of the quantized network and the 32-bit pre-trained network. The structural features are obtained from the last layer of the high-level feature extractor. The balancing weight  $\lambda$  is set as 1000 in our experiments. Also, the weight  $\lambda_V$  to balance  $\mathcal{L}_V$  and  $\mathcal{L}_R$  in Eq. 3 is set differently depending on the mismatch severeness of the SR architecture. We provide detailed settings in the supplementary materials.

## 4 Experiments

The efficacy and adaptability of the proposed quantization framework ODM are assessed through its application to several SR networks. The experimental settings are outlined (Sec. 4.1), and both quantitative (Sec. 4.2) and qualitative (Sec. 4.3) evaluations are conducted on various SR networks. Furthermore, ablation experiments are conducted to examine each component of the framework in detail (Sec. 4.4).

### 4.1 Implementation details

**Models and training.** The proposed framework is applied directly to existing representative SR networks that produce satisfactory SR results but with heavy computations: EDSR (baseline) [33], RDN [47], and SRResNet [29]. Following existing works on SR quantization [30, 36, 43, 17, 48, 16],

Table 1: **Quantitative comparisons on EDSR** of scale 4.

Model	Bit	Set5		Set14		B100		Urban100	
		PSNR	SSIM	PSNR	SSIM	PSNR	SSIM	PSNR	SSIM
EDSR [33]	32	32.10	0.894	28.58	0.781	27.56	0.736	26.04	0.785
EDSR-PAMS [30]	4	31.59	0.885	28.20	0.773	27.32	0.728	25.32	0.762
EDSR-DAQ [17]	4	31.85	0.887	28.38	0.776	27.42	0.732	25.73	0.772
EDSR-DDTB [48]	4	31.85	0.889	28.39	0.777	27.44	0.732	25.69	0.774
EDSR-ODM (Ours)	4	<b>32.03</b>	<b>0.891</b>	<b>28.48</b>	<b>0.779</b>	<b>27.49</b>	<b>0.735</b>	<b>25.79</b>	<b>0.778</b>
EDSR-PAMS [30]	3	27.25	0.780	25.24	0.673	25.38	0.644	22.76	0.641
EDSR-DAQ [17]	3	31.66	0.884	28.19	0.771	27.28	0.728	25.40	0.762
EDSR-DDTB [48]	3	31.52	0.883	28.18	0.771	27.30	0.727	25.33	0.761
EDSR-ODM (Ours)	3	<b>31.80</b>	<b>0.888</b>	<b>28.35</b>	<b>0.776</b>	<b>27.41</b>	<b>0.732</b>	<b>25.52</b>	<b>0.770</b>
EDSR-PAMS [30]	2	29.51	0.835	26.79	0.734	26.45	0.696	23.72	0.688
EDSR-DAQ [17]	2	31.01	0.871	27.89	0.762	27.09	0.719	24.88	0.740
EDSR-DDTB [48]	2	30.97	0.876	27.87	0.764	27.09	0.719	24.82	0.742
EDSR-ODM (Ours)	2	<b>31.49</b>	<b>0.883</b>	<b>28.12</b>	<b>0.770</b>	<b>27.26</b>	<b>0.727</b>	<b>25.15</b>	<b>0.756</b>

Table 2: **Quantitative comparisons on RDN** of scale 4.

Model	Bit	Set5		Set14		B100		Urban100	
		PSNR	SSIM	PSNR	SSIM	PSNR	SSIM	PSNR	SSIM
RDN [47]	32	32.24	0.896	28.67	0.784	27.63	0.738	26.29	0.792
RDN-PAMS [30]	4	30.44	0.862	27.54	0.753	26.87	0.710	24.52	0.726
RDN-DAQ [17]	4	31.91	0.889	28.38	0.775	27.38	0.733	25.81	0.779
RDN-DDTB [48]	4	31.97	0.891	28.49	0.780	27.49	0.735	25.90	0.783
RDN-ODM (Ours)	4	<b>32.03</b>	<b>0.892</b>	<b>28.51</b>	<b>0.780</b>	<b>27.54</b>	<b>0.736</b>	<b>25.92</b>	<b>0.784</b>
RDN-PAMS [30]	3	29.54	0.838	26.82	0.734	26.47	0.696	23.83	0.692
RDN-DAQ [17]	3	31.57	0.883	28.18	0.771	27.27	0.728	25.47	0.765
RDN-DDTB [48]	3	31.49	0.883	28.17	0.772	27.30	0.728	25.35	0.764
RDN-ODM (Ours)	3	<b>31.56</b>	<b>0.884</b>	<b>28.21</b>	<b>0.773</b>	<b>27.33</b>	<b>0.730</b>	<b>25.37</b>	<b>0.765</b>
RDN-PAMS [30]	2	29.73	0.843	26.96	0.739	26.57	0.700	23.87	0.696
RDN-DAQ [17]	2	30.71	0.866	27.61	0.755	26.93	0.715	24.71	0.731
RDN-DDTB [48]	2	30.57	0.867	27.56	0.757	26.91	0.714	24.50	0.728
RDN-ODM (Ours)	2	<b>30.98</b>	<b>0.873</b>	<b>27.79</b>	<b>0.762</b>	<b>27.05</b>	<b>0.719</b>	<b>24.74</b>	<b>0.737</b>

weights and activations of the high-level feature extraction module are quantized which is the most computationally-demanding. Training and validation are done with DIV2K [1] dataset. ODM trains the network for 60 epochs, with  $1 \times 10^{-4}$  initial learning rate that is halved every 15 epochs and with a batch size of 8. All our experiments are implemented with PyTorch and run using a single RTX 2080Ti GPU.

**Evaluation.** We evaluate our framework on the standard benchmark (Set5 [4], Set14 [29], BSD100 [37], and Urban100 [19]). We report peak signal-to-noise ratio (PSNR) and structural similarity index (SSIM [42]) to evaluate the SR performance. To evaluate the computational complexity of our framework, we measure the BitOPs and storage size. BitOPs is the number of operations that are weighted by the bit-widths of the two operands. Storage size is the number of stored parameters weighted by the precision of each parameter value. Furthermore, our ablation study is conducted on EDSR of scale 4 with 2-bit setting.

## 4.2 Quantitative results

To evaluate the effectiveness of our proposed scheme, we compare the results with existing SR quantization works PAMS [30], DAQ [17], and DDTB [48] using the official code. To make a fair comparison with the existing works, we reproduce the results of other methods using the same training epochs. As shown in Table 1, our framework ODM outperforms other methods largely for all 4, 3, and 2-bit, and notably, the improvement is significant for 2-bit quantization. Also, 4-bit EDSR-ODM achieves closer accuracy to the 32-bit EDSR, where the margin is only 0.07dB for Set5. This indicates

Table 3: **Quantitative comparisons on SRResNet** of scale 4.

Model	Bit	Set5		Set14		B100		Urban100	
		PSNR	SSIM	PSNR	SSIM	PSNR	SSIM	PSNR	SSIM
SRResNet [29]	32	32.07	0.893	28.50	0.780	27.52	0.735	25.86	0.779
SRResNet-PAMS [30]	4	31.88	0.891	28.41	0.777	27.45	0.732	25.68	0.773
SRResNet-DAQ [17]	4	31.85	0.889	28.41	0.777	27.45	0.732	25.70	0.772
SRResNet-DDTB [48]	4	31.97	0.892	28.46	0.778	27.48	0.733	25.77	0.776
SRResNet-ODM (Ours)	4	<b>32.00</b>	<b>0.892</b>	<b>28.46</b>	<b>0.778</b>	<b>27.48</b>	<b>0.734</b>	<b>25.77</b>	<b>0.776</b>
SRResNet-PAMS [30]	3	31.68	0.888	28.27	0.774	26.79	0.709	25.46	0.765
SRResNet-DAQ [17]	3	31.81	0.889	28.35	0.776	27.40	0.733	25.63	0.772
SRResNet-DDTB [48]	3	31.85	0.890	28.39	0.776	27.44	0.731	25.64	0.770
SRResNet-ODM (Ours)	3	<b>31.86</b>	<b>0.890</b>	<b>28.39</b>	<b>0.776</b>	<b>27.44</b>	<b>0.732</b>	<b>25.65</b>	<b>0.771</b>
SRResNet-PAMS [30]	2	30.25	0.861	27.36	0.750	26.79	0.709	24.19	0.713
SRResNet-DAQ [17]	2	31.57	0.886	28.19	0.773	27.30	0.729	25.39	0.765
SRResNet-DDTB [48]	2	31.51	0.887	28.23	0.773	27.33	0.728	25.37	0.762
SRResNet-ODM (Ours)	2	<b>31.59</b>	<b>0.887</b>	<b>28.27</b>	<b>0.773</b>	<b>27.36</b>	<b>0.729</b>	<b>25.44</b>	<b>0.765</b>

Table 4: **Computational complexity comparison** with SR quantization methods on EDSR ( $\times 4$ ).

Model	Bit	Storage size	BitOPs	PSNR	SSIM
EDSR [33]	32	1517.6K	527.1T	32.10	0.894
EDSR-PAMS [30]	2	411.7K	215.1T	29.51	0.835
EDSR-DAQ [17]	2	411.7K	216.1T	31.01	0.871
EDSR-DDTB [48]	2	413.4K	215.1T	30.97	0.876
EDSR-ODM (Ours)	2	<b>411.7K</b>	<b>215.1T</b>	<b>31.49</b>	<b>0.883</b>

that ODM can effectively bridge the gap between the quantized network and the floating-point network. Also, Table 2 compares the results on RDN. The results show that ODM achieves consistently superior performance on 4, 3, and 2-bit quantization.

Furthermore, we evaluate our framework also on SRResNet which is shown in Table 3. SRResNet architecture includes BN layers and thus the distribution mismatch problem is not as severe as in EDSR or RDN. Nevertheless, ODM is also proven effective for quantizing SRResNet on all bit settings, showing slightly better performance than the existing quantization methods. Additional experiments that further demonstrate the applicability of ODM are provided in the supplementary materials.

Along with the SR accuracy, we also compare the computational complexity of our framework in Table 4. We calculate the BitOPs for generating a  $1920 \times 1080$  image. Overall, our framework ODM achieves higher accuracy (PSNR/SSIM) with similar or less computational resources. As reported in Table 5, the distribution offsets incur minimal computational overhead. On EDSR, distribution offsets involve an additional 0.02% storage size and the offset scaling and shifting involves 0.005% additional BitOPs. Compared to existing works that utilize dynamic adaptation, the computational overhead is  $\times 30$  smaller in storage size than DDTB [48] and  $\times 100$  smaller in BitOPs than DAQ [17].

### 4.3 Qualitative results

Figure 4 provides qualitative results and comparisons with the output images from quantized EDSR and RDN. Our method, ODM, produces a further visually clean output image compared to existing quantization methods. In contrast, existing methods, especially PAMS, suffer from blurred lines or artifacts. The qualitative results stress the importance of alleviating the distribution mismatch problem in SR networks. More results are provided in the supplementary materials.

### 4.4 Ablation study

On EDSR 2-bit setting, we verify the importance of each attribute of our framework: cooperative variance regularization and distribution offsets. As shown in Table 5, both cooperative variance



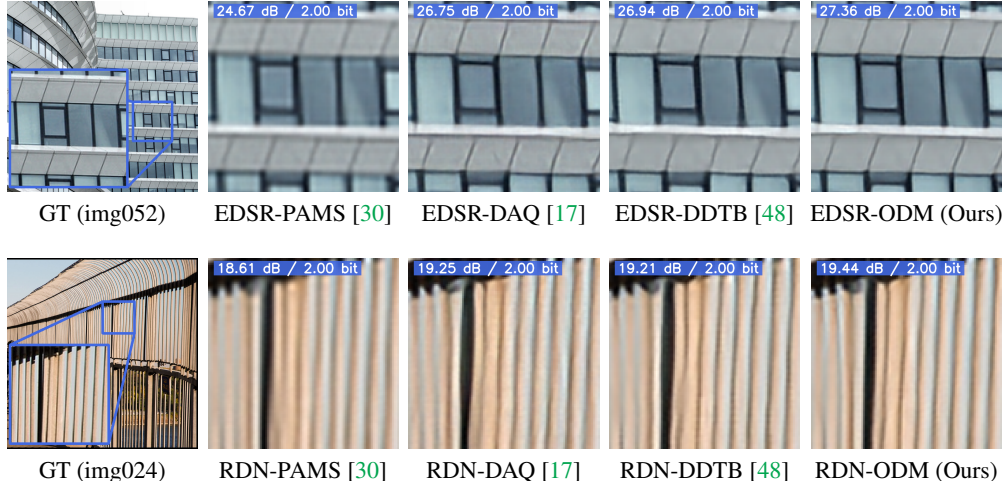


Figure 4: **Qualitative results** on Urban100 with EDSR and RDN-based models.

Table 5: **Ablation study on each attribute of our framework.** Var. Reg. refers to the variance regularization loss and Coop. denotes whether the cooperative variance regularization is utilized or not, and Dist. Off. refers to the distribution offsets. Percentage in brackets denotes the additional computation compared to the baseline.

Model	Coop.	Var. Reg.	Dist. Off.	Storage size	BitOPs	PSNR	SSIM
EDSR-PAMS [30]	-	-	-	411.7K	215.0T	29.51	0.835
(a)	-	✓	-	-	-	31.08	0.872
(b)	✓	✓	-	-	-	31.31	0.879
(c)	-	-	✓	+0.08K (+0.02%)	+0.01T (+0.005%)	31.44	0.882
<b>EDSR-ODM</b>	✓	✓	✓	+0.08K (+0.02%)	+0.01T (+0.005%)	31.49	0.883

regularization and distribution offsets can respectively improve the baseline accuracy. Compared to using variance regularization directly (a), our cooperative scheme (b) improves the SR accuracy (+0.23dB). Although leveraging distribution offsets (c) incurs additional computations, it largely increases the accuracy and the computational overhead is minimal. The two components can jointly reduce the distribution mismatch and result in a further accurate quantized SR network.

## 5 Conclusion

SR networks suffer accuracy loss from quantization due to the inherent distribution mismatch of the features. Instead of adapting resource-demanding dynamic modules to handle distinct distributions during test time, we introduce a new quantization-aware training technique that relieves the mismatch problem via distribution optimization. We leverage variance regularization loss that updates the SR network towards being quantization-friendly and also accurately super-resolving images. Also, through analysis of the distribution mismatch of different layers, we find that applying additional shifting offsets to layers with a large mismatch in terms of shift and scaling offsets to the layers with a large scaling mismatch can further reduce the distribution mismatch issue with minimal computational overhead. Experimental results demonstrate that the proposed training scheme achieves superior performance in terms of accuracy and computational complexity on various SR networks.

**Limitation** Our framework shows limited effectiveness for SR networks with batch normalization (BN) layers, such as SRResNet. This is because BN layers relieve the variation in feature distribution, thus the distribution mismatch problem is not as severe.

## References

- [1] Eirikur Agustsson and Radu Timofte. NTIRE 2017 challenge on single image super-resolution: Dataset and study. In *CVPR Workshops*, 2017. 7
- [2] Mustafa Ayazoglu. Extremely lightweight quantization robust real-time single-image super resolution for mobile devices. In *CVPR Workshops*, 2021. 3
- [3] Yoshua Bengio, Nicholas Léonard, and Aaron Courville. Estimating or propagating gradients through stochastic neurons for conditional computation. *arXiv preprint arXiv:1308.3432*, 2013. 4
- [4] Marco Bevilacqua, Aline Roumy, Christine Guillemot, and Marie Line Alberi-Morel. Low-complexity single-image super-resolution based on nonnegative neighbor embedding. In *BMVC*, 2012. 7
- [5] Zhaowei Cai and Nuno Vasconcelos. Rethinking differentiable search for mixed-precision neural networks. In *CVPR*, 2020. 3
- [6] Zhaowei Cai, Xiaodong He, Jian Sun, and Nuno Vasconcelos. Deep learning with low precision by half-wave gaussian quantization. In *CVPR*, 2017. 3
- [7] Jungwook Choi, Zhuo Wang, Swagath Venkataramani, Pierce I-Jen Chuang, Vijayalakshmi Srinivasan, and Kailash Gopalakrishnan. Pact: Parameterized clipping activation for quantized neural networks. *arXiv preprint arXiv:1805.06085*, 2018. 1, 3
- [8] Xiangxiang Chu, Bo Zhang, Hailong Ma, Ruijun Xu, and Qingyuan Li. Fast, accurate and lightweight super-resolution with neural architecture search. In *ICPR*, 2021. 2
- [9] Chao Dong, Chen Change Loy, Kaiming He, and Xiaoou Tang. Learning a deep convolutional network for image super-resolution. In *ECCV*, 2014. 2
- [10] Chao Dong, Chen Change Loy, Kaiming He, and Xiaoou Tang. Image super-resolution using deep convolutional networks. *IEEE TPAMI*, 38(2):295–307, 2015. 1
- [11] Zhen Dong, Zhewei Yao, Amir Gholami, Michael W Mahoney, and Kurt Keutzer. Hawq: Hessian aware quantization of neural networks with mixed-precision. In *ICCV*, 2019. 3
- [12] Yunshu Du, Wojciech M Czarnecki, Siddhant M Jayakumar, Mehrdad Farajtabar, Razvan Pascanu, and Balaji Lakshminarayanan. Adapting auxiliary losses using gradient similarity. *arXiv preprint arXiv:1812.02224*, 2018. 4
- [13] Steven K Esser, Jeffrey L McKinstry, Deepika Bablani, Rathinakumar Appuswamy, and Dharmendra S Modha. Learned step size quantization. In *ICLR*, 2020. 3
- [14] Amir Gholami, Sehoon Kim, Zhen Dong, Zhewei Yao, Michael W Mahoney, and Kurt Keutzer. A survey of quantization methods for efficient neural network inference. *arXiv preprint arXiv:2103.13630*, 2021. 3
- [15] Hai Victor Habi, Roy H Jennings, and Arnon Netzer. Hmq: Hardware friendly mixed precision quantization block for cnns. In *ECCV*, 2020. 3
- [16] Cheeun Hong, Sungyong Baik, Heewon Kim, Seungjun Nah, and Kyoung Mu Lee. Cadyq: Content-aware dynamic quantization for image super-resolution. In *ECCV*, 2022. 3, 6
- [17] Cheeun Hong, Heewon Kim, Sungyong Baik, Junghun Oh, and Kyoung Mu Lee. Daq: Channel-wise distribution-aware quantization for deep image super-resolution networks. In *WACV*, 2022. 2, 3, 4, 6, 7, 8, 9
- [18] Lu Hou and James T. Kwok. Loss-aware weight quantization of deep networks. In *ICLR*, 2018. 1
- [19] Jia-Bin Huang, Abhishek Singh, and Narendra Ahuja. Single image super-resolution from transformed self-exemplars. In *CVPR*, 2015. 7

- [20] Zheng Hui, Xiumei Wang, and Xinbo Gao. Fast and accurate single image super-resolution via information distillation network. In *CVPR*, 2018. 2
- [21] Zheng Hui, Xinbo Gao, Yunchu Yang, and Xiumei Wang. Lightweight image super-resolution with information multi-distillation network. In *ACMMM*, 2019. 2
- [22] Andrey Ignatov, Radu Timofte, Maurizio Denna, and Abdel Younes. Real-time quantized image super-resolution on mobile npus, mobile ai 2021 challenge: Report. In *CVPR Workshops*, 2021. 1, 3
- [23] Xinrui Jiang, Nannan Wang, Jingwei Xin, Keyu Li, Xi Yang, and Xinbo Gao. Training binary neural network without batch normalization for image super-resolution. In *AAAI*, 2021. 3
- [24] Qing Jin, Linjie Yang, and Zhenyu Liao. Adabits: Neural network quantization with adaptive bit-widths. In *CVPR*, 2020. 3
- [25] Younghyun Jo and Seon Joo Kim. Practical single-image super-resolution using look-up table. In *CVPR*, 2021. 2
- [26] Sangil Jung, Changyong Son, Seohyung Lee, Jinwoo Son, Jae-Joon Han, Youngjun Kwak, Sung Ju Hwang, and Changkyu Choi. Learning to quantize deep networks by optimizing quantization intervals with task loss. In *CVPR*, 2019. 3
- [27] Heewon Kim, Seokil Hong, Bohyung Han, Heesoo Myeong, and Kyoung Mu Lee. Fine-grained neural architecture search. *arXiv preprint arXiv:1911.07478*, 2019. 2
- [28] Jiwon Kim, Jungkwon Lee, and Kyoung Mu Lee. Accurate image super-resolution using very deep convolutional networks. In *CVPR*, 2016. 1
- [29] Christian Ledig, Lucas Theis, Ferenc Huszar, Jose Caballero, Andrew Cunningham, Alejandro Acosta, Andrew Aitken, Alykhan Tejani, Johannes Totz, Zehan Wang, and Wenzhe Shi. Photo-realistic single image super-resolution using a generative adversarial network. In *CVPR*, 2017. 2, 6, 7, 8
- [30] Huixia Li, Chenqian Yan, Shaohui Lin, Xiawu Zheng, B. Zhang, F. Yang, and Rongrong Ji. Pams: Quantized super-resolution via parameterized max scale. In *ECCV*, 2020. 2, 3, 4, 6, 7, 8, 9
- [31] Yawei Li, Shuhang Gu, Kai Zhang, Luc Van Gool, and Radu Timofte. Dhp: Differentiable meta pruning via hypernetworks. In *ECCV*, 2020. 2
- [32] Yawei Li, Wen Li, Martin Danelljan, Kai Zhang, Shuhang Gu, Luc Van Gool, and Radu Timofte. The heterogeneity hypothesis: Finding layer-wise differentiated network architectures. In *CVPR*, 2021. 2
- [33] Bee Lim, Sanghyun Son, Heewon Kim, Seungjun Nah, and Kyoung Mu Lee. Enhanced deep residual networks for single image super-resolution. In *CVPR Workshops*, 2017. 1, 2, 4, 5, 6, 7, 8
- [34] Jingyu Liu, Qiong Wang, Dunbo Zhang, and Li Shen. Super-resolution model quantized in multi-precision. *Electronics*, 10(17):2176, 2021. 3
- [35] Qian Lou, Feng Guo, Lantao Liu, Minje Kim, and Lei Jiang. AutoQ: Automated kernel-wise neural network quantization. In *ICLR*, 2020. 3
- [36] Yinglan Ma, Hongyu Xiong, Zhe Hu, and Lizhuang Ma. Efficient super resolution using binarized neural network. In *CVPR Workshops*, 2019. 3, 6
- [37] David Martin, Charless Fowlkes, Doron Tal, and Jitendra Malik. A database of human segmented natural images and its application to evaluating segmentation algorithms and measuring ecological statistics. In *Proceedings Eighth IEEE International Conference on Computer Vision. ICCV 2001*, volume 2, pages 416–423. IEEE, 2001. 7
- [38] Junghun Oh, Heewon Kim, Seungjun Nah, Cheeun Hong, Jonghyun Choi, and Kyoung Mu Lee. Attentive fine-grained structured sparsity for image restoration. In *CVPR*, 2022. 2

- [39] Dehua Song, Chang Xu, Xu Jia, Yiyi Chen, Chunjing Xu, and Yunhe Wang. Efficient residual dense block search for image super-resolution. In *AAAI*, 2020. 2
- [40] Hu Wang, Peng Chen, Bohan Zhuang, and Chunhua Shen. Fully quantized image super-resolution networks. In *ACMMM*, 2021. 3
- [41] Kuan Wang, Zhijian Liu, Yujun Lin, Ji Lin, and Song Han. Haq: Hardware-aware automated quantization with mixed precision. In *CVPR*, 2019. 3
- [42] Zhou Wang, Alan C Bovik, Hamid R Sheikh, Eero P Simoncelli, et al. Image quality assessment: from error visibility to structural similarity. *IEEE TIP*, 13(4):600–612, 2004. 7
- [43] Jingwei Xin, Nannan Wang, Xinrui Jiang, Jie Li, Heng Huang, and Xinbo Gao. Binarized neural network for single image super resolution. In *ECCV*, 2020. 3, 6
- [44] Linjie Yang and Qing Jin. Fracbits: Mixed precision quantization via fractional bit-widths. In *AAAI*, 2021. 3
- [45] Yiman Zhang, Hanting Chen, Xinghao Chen, Yiping Deng, Chunjing Xu, and Yunhe Wang. Data-free knowledge distillation for image super-resolution. In *CVPR*, 2021. 2
- [46] Yulun Zhang, Kunpeng Li, Kai Li, Lichen Wang, Bineng Zhong, and Yun Fu. Image super-resolution using very deep residual channel attention networks. In *ECCV*, 2018. 1, 2
- [47] Yulun Zhang, Yapeng Tian, Yu Kong, Bineng Zhong, and Yun Fu. Residual dense network for image super-resolution. In *CVPR*, 2018. 1, 6, 7
- [48] Yunshan Zhong, Mingbao Lin, Xunchao Li, Ke Li, Yunhang Shen, Fei Chao, Yongjian Wu, and Rongrong Ji. Dynamic dual trainable bounds for ultra-low precision super-resolution networks. In *ECCV*, 2022. 2, 3, 4, 6, 7, 8, 9
- [49] Shuchang Zhou, Yuxin Wu, Zekun Ni, Xinyu Zhou, He Wen, and Yuheng Zou. DoReFa-Net: Training low bitwidth convolutional neural networks with low bitwidth gradients. *arXiv preprint arXiv:1606.06160*, 2016. 1, 3
- [50] Bohan Zhuang, Chunhua Shen, Mingkui Tan, Lingqiao Liu, and Ian Reid. Towards effective low-bitwidth convolutional neural networks. In *CVPR*, 2018. 3

---

# Supplementary Material for “Overcoming Distribution Mismatch in Quantizing Image Super-Resolution Networks”

---

**Cheun Hong**  
Dept. of ECE & ASRI,  
Seoul National University  
cheun914@snu.ac.kr

**Kyoung Mu Lee**  
IPAI, Dept. of ECE & ASRI,  
Seoul National University  
kyoungmu@snu.ac.kr

In this supplementary material, we present the implementation details of our training framework, ODM in Section S1; additional experimental results in Section S2; additional complexity analysis in Section S3; additional qualitative results in Section S4.

## S1 Implementation details

$\lambda_V$ , the balance weight between reconstruction loss and variance regularization loss, is set differently based on the backbone model. We set  $\lambda_V$ , as  $1 \times 10^{-4}$  for EDSR and SRResNet, and  $1 \times 10^{-5}$  for RDN, which is a larger model with more convolutional layers than EDSR and SRResNet. Since  $\mathcal{L}_V$  is sum of the variances in features of all the convolutional layers, it is natural to leverage smaller  $\lambda_V$  for larger models.

## S2 Additional experiments

In addition to the comparisons of the main manuscript done on SR networks of scale  $\times 4$ , we evaluate our framework on networks of scale  $\times 2$ . As shown in Table S1, our framework outperforms existing SR quantization methods in terms of both PSNR and SSIM, demonstrating the effectiveness of our approach on scale 2 SR networks. Specifically, the PSNR gain on Set5 is 0.37 dB on EDSR and 0.37 dB on RDN, while it is 0.06 dB on SRResNet, as the distribution mismatch problem is particularly trivial for SRResNet.

Table S1: Quantitative comparisons on SR networks of scale  $\times 2$ .

Model	Bit	Set5		Set14		B100		Urban100	
		PSNR	SSIM	PSNR	SSIM	PSNR	SSIM	PSNR	SSIM
EDSR [33]	32	37.93	0.960	33.46	0.916	32.10	0.899	31.71	0.925
EDSR-PAMS [30]	2	35.30	0.946	31.63	0.899	30.66	0.879	28.11	0.875
EDSR-DDTB [48]	2	37.25	0.958	32.87	0.911	31.67	0.893	30.34	0.910
EDSR-ODM (Ours)	2	<b>37.62</b>	<b>0.959</b>	<b>33.14</b>	<b>0.914</b>	<b>31.88</b>	<b>0.896</b>	<b>30.92</b>	<b>0.917</b>
RDN [47]	32	38.05	0.961	33.59	0.917	32.20	0.900	32.13	0.927
RDN-PAMS [30]	2	35.45	0.946	31.67	0.899	30.69	0.879	28.14	0.874
RDN-DDTB [48]	2	36.76	0.955	32.54	0.908	31.44	0.890	29.77	0.903
RDN-ODM (Ours)	2	<b>37.13</b>	<b>0.957</b>	<b>32.69</b>	<b>0.910</b>	<b>31.53</b>	<b>0.892</b>	<b>29.92</b>	<b>0.904</b>
SRResNet [29]	32	37.89	0.960	33.40	0.916	32.08	0.898	31.60	0.923
SRResNet-PAMS [30]	2	34.75	0.942	31.31	0.896	30.48	0.877	27.86	0.868
SRResNet-DDTB [48]	2	37.46	0.958	33.02	0.913	31.78	0.895	30.57	0.913
SRResNet-ODM (Ours)	2	<b>37.52</b>	<b>0.959</b>	<b>33.02</b>	<b>0.913</b>	<b>31.79</b>	<b>0.895</b>	<b>30.55</b>	<b>0.913</b>

Moreover, we compare our method with fully-quantized SR networks, EDSR-FQSR [40], which quantizes all layers and also the skip-connections. To make a fair comparison, we also quantize all convolutional layers and the skip-connections. In Table S2, the results demonstrate that ODM is also effective when the network is fully quantized.

Table S2: **Quantitative comparisons on EDSR with fully quantized methods.** S.C. refers to the bit-width of skip-connections.

Scale	Model	Bit	S.C.	Set5		Set14		B100		Urban100	
				PSNR	SSIM	PSNR	SSIM	PSNR	SSIM	PSNR	SSIM
×4	EDSR [33]	32	32	32.10	0.894	28.58	0.781	27.56	0.736	26.04	0.785
	EDSR-FQSR [40]	4	8	30.93	0.870	27.82	0.761	27.07	0.715	24.93	0.744
	EDSR-DDTB [48]	4	8	31.91	0.889	28.40	0.777	27.44	0.732	25.70	0.775
	EDSR-ODM (Ours)	4	8	<b>32.02</b>	<b>0.891</b>	<b>28.46</b>	<b>0.778</b>	<b>27.48</b>	<b>0.734</b>	<b>25.76</b>	<b>0.777</b>
×2	EDSR [33]	32	32	37.93	0.960	33.46	0.916	32.10	0.899	31.71	0.925
	EDSR-FQSR [40]	4	8	37.04	0.951	32.84	0.908	31.67	0.889	30.65	0.911
	EDSR-DDTB [48]	4	8	37.83	0.960	33.44	0.916	32.07	0.898	31.60	0.924
	EDSR-ODM (Ours)	4	8	<b>37.87</b>	<b>0.960</b>	<b>33.43</b>	<b>0.915</b>	<b>32.10</b>	<b>0.899</b>	<b>31.75</b>	<b>0.925</b>

### S3 Additional complexity comparison

Along with the EDSR backbone models analyzed in the main manuscript, we present computational complexity analyses on RDN and SRResNet-based models. We measure BitOPs for generating a  $(1920 \times 1080)$  image and storage size required to store the model weights. As shown in Table S3, our framework achieves higher reconstruction accuracy regarding PSNR and SSIM, with less or similar storage size and BitOPs. In particular, RDN-ODM involves ×4 smaller storage size overhead than RDN-DDTB, and ×800 fewer BitOPs overhead than RDN-DAQ, while the PSNR gap is 0.41dB or higher. Although the PSNR gap is smaller on SRResNet, ODM still achieves higher PSNR with fewer computations than DAQ and DDTB. Compared to PAMS, our framework incurs additional storage size on RDN (0.7%) and SRResNet (0.1%), but the accuracy gap with PAMS is significant ( $\sim 1.4$  dB).

Table S3: **Computational complexity comparison** with SR quantization methods on RDN and SRResNet (×4).

Model	Bit	Storage size	BitOPs	PSNR	SSIM
RDN [47]	32	22271.1K	6032.9T	32.24	0.896
RDN-PAMS [30]	2	1715.9K	236.6T	29.54	0.838
RDN-DAQ [17]	2	1715.9K	287.7T	30.33	0.858
RDN-DDTB [48]	2	1769.7K	236.6T	30.57	0.867
RDN-ODM (Ours)	2	<b>1727.9K</b>	<b>236.6T</b>	<b>30.98</b>	<b>0.871</b>
SRResNet [29]	32	1546.8K	588.8T	32.10	0.894
SRResNet-PAMS [30]	2	440.9K	276.9T	30.25	0.861
SRResNet-DAQ [17]	2	440.9K	279.0T	31.57	0.886
SRResNet-DDTB [48]	2	442.3K	276.9T	31.51	0.887
SRResNet-ODM (Ours)	2	<b>441.4K</b>	<b>276.9T</b>	<b>31.59</b>	<b>0.887</b>

## S4 Additional qualitative results

We show more visual comparisons in Figure S1. Overall, while other methods suffer from blurred lines or damaged structures in test images (Urban100), our approach produces further clear lines and structures. These results demonstrate that our ODM is beneficial quantitatively and qualitatively.

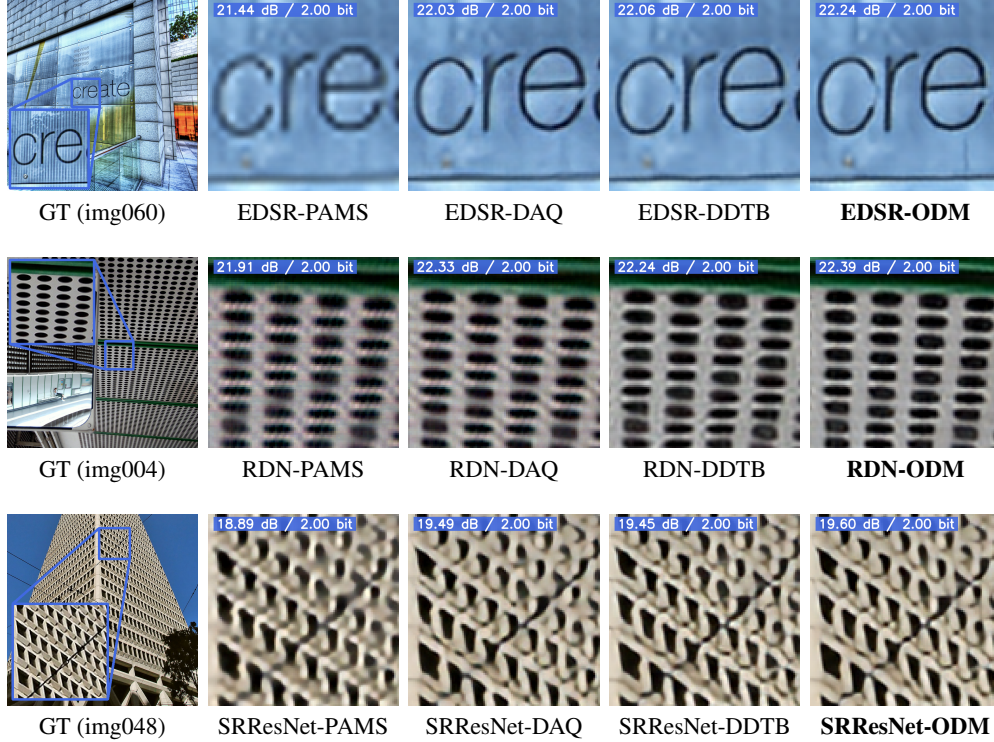


Figure S1: **Qualitative results** on EDSR, RDN, and SRResNet of scale 4.

### License of the Used Assets

- DIV2K [1] dataset is publicly available for academic research purposes.
- Set5 [4], Set14 [29], BSD100 [37], Urban100 [19] datasets are made available at <https://github.com/jbhuang0604/SelfExSR>.